

# Involvement of p38 $\alpha$ in the mitotic progression of *p53*<sup>-/-</sup> tetraploid cells

Ilio Vitale,<sup>1,3,†</sup> Mohamed Jemaà,<sup>1,3,†</sup> Laura Senovilla,<sup>1,3</sup> Lorenzo Galluzzi,<sup>1,3</sup> Santiago Rello-Varona,<sup>1,3</sup> Didier Metivier,<sup>1,3</sup> Hugues Ripoche,<sup>2,4-6</sup> Vladimir Lazar,<sup>2,4-6</sup> Philippe Dessen,<sup>2,4-6</sup> Maria Castedo<sup>1-3,‡,\*</sup> and Guido Kroemer<sup>1-3,‡,\*</sup>

<sup>1</sup>INSERM; U848; Villejuif, France; <sup>2</sup>Institut Gustave Roussy; Villejuif, France; <sup>3</sup>Université Paris Sud-XI; Villejuif, France; <sup>4</sup>Institut Gustave Roussy; Unité de Génomique Fonctionnelle et Bioinformatique; Villejuif, France; <sup>5</sup>Institut Gustave Roussy; IFR54; Villejuif, France; <sup>6</sup>Centre National de la Recherche Scientifique; FRE2939; Villejuif, France

<sup>†</sup>These authors contributed equally to this work.

<sup>‡</sup>These authors share senior coauthorship.

**Key words:** aneuploidy, apoptosis, centrosome, colon carcinoma, MOS

The tumor suppressor protein p53 plays a major role in preserving genomic stability. p53 suppresses a pathway leading from normal diploidy to neoplastic aneuploidy (via an intermediate metastable stage of tetraploidy) at two levels: first by preventing the generation/survival of tetraploid cells, and second by repressing their aberrant multipolar division. Here, we report the characterization of *p53*<sup>-/-</sup> tetraploid cells, which—at difference with both their *p53*<sup>-/-</sup> diploid and their *p53*<sup>+/+</sup> tetraploid counterparts—manifest a marked hyperphosphorylation of the mitogen-activated protein kinase MAPK14 (best known as p38 $\alpha$ ) that is particularly strong during mitosis. In *p53*<sup>-/-</sup> tetraploid cells, phosphorylated p38 $\alpha$  accumulated at centrosomes during the metaphase and at midbodies during the telophase. Selective knockdown or pharmacological inhibition of p38 $\alpha$  had a dramatic effect on *p53*<sup>-/-</sup> (but not *p53*<sup>+/+</sup>) tetraploids, causing the activation of the spindle assembly checkpoint, an arrest during the metaphase, a major increase in abnormal bipolar and monopolar mitoses, as well as an increment in the generation of multinuclear cells. We conclude that the mitotic progression of *p53*<sup>-/-</sup> (but not *p53*<sup>+/+</sup>) tetraploids heavily relies on p38 $\alpha$ , revealing a novel function for this protein in the context of aneuploidizing cell divisions.

Do not distribute.

## Introduction

Tetraploidy can constitute a metastable intermediate between healthy diploidy and neoplastic aneuploidy. Tetraploidy is detected in many cancers as well as in some precancerous lesions such as cervical metaplasia or Barrett's esophagus, where its presence is associated with the inactivation of the tumor suppressor p53.<sup>1,2</sup> The inactivation of numerous tumor suppressor proteins such as p53,<sup>3</sup> APC,<sup>4</sup> BRCA1<sup>5</sup> and LATS2<sup>6</sup> can cause tetraploidy or facilitate its induction, for instance in the context of telomerase insufficiency<sup>7</sup> or microtubular inhibition.<sup>8</sup> For example, the depletion or deletion of APC causes tetraploidization in vitro, in cultured cells, as well as in vivo, in jejunal epithelial cells.<sup>9,10</sup> Moreover, the inactivation of p53 in cancer cell lines or mammalian epithelial cells facilitates the survival of tetraploids that are generated by the suppression of cytokinesis or karyokinesis.<sup>8,11-15</sup> Conversely, several oncoproteins including Aurora A,<sup>16</sup> MYC,<sup>17</sup> and HPV-virus encoded E6<sup>18</sup> can stimulate tetraploidization.

Newly generated tetraploid cells can either undergo apoptosis after a latency, form a stable tetraploid clone or engage in a process of multipolar division that culminates in the simultaneous generation of three or more daughter cells.<sup>8,19</sup> This entails

the stochastic distribution of chromosomes, in turn precluding further cell divisions because nullisomies (the total absence of one particular chromosome) and polysomies (the presence of one or more extra chromosomes) are always and most often lethal, respectively.<sup>20-22</sup> Still, in exceptional cases, daughter cells arising from multipolar divisions survive and yield an aneuploid progeny. Indeed, when *p53*<sup>-/-</sup> tetraploid clones are cultured for a prolonged period, they tend to accumulate an ever-increasing subpopulation of pseudo-diploid cells, which have been formed through multipolar divisions.<sup>23</sup> We have recently demonstrated that multipolar mitoses (which reduce the tetraploid genome to a sub-tetraploid, often near-to-diploid, one) are favored by the inactivation of p53, be it by the deletion of *TP53* (knockout by homologous recombination), protein depletion (knockdown by small interfering RNAs) or inhibition (with pharmacological agents). In addition, we found that the overexpression of *MOS* favors multipolar, asymmetric cell divisions and the conversion of tetraploid into aneuploid cells.<sup>23</sup> Thus, oncogenes and tumor suppressor genes intervene in the pathway that links diploidy to aneuploidy (via tetraploidy) at least at two levels. First they control the propensity of tetraploids to be formed (and to survive). Second, they affect the frequency of multipolar divisions that can

\*Correspondence to: Guido Kroemer and Maria Castedo; Email: kroemer@orange.fr and castedo@igr.fr

Submitted: 04/28/10; Accepted: 05/03/10

Previously published online: [www.landesbioscience.com/journals/cc/article/12248](http://www.landesbioscience.com/journals/cc/article/12248)

DOI: 10.4161/cc.9.14.12248

reduce 'normal' tetraploidy (with tetrasomy of all chromosomes) to a potentially neoplastic, aneuploid state.

The mitogen-activated protein kinase MAPK14 (also known as p38 $\alpha$  or stress-activated protein kinase 2A, SAPK2A) is triggered by multiple stressors including UV light,<sup>24</sup> heat,<sup>25</sup> osmotic shock,<sup>26,27</sup> DNA damage<sup>28</sup> and deregulation of the cell cycle, for instance upon the loss of centrosome integrity.<sup>29</sup> p38 $\alpha$  can directly phosphorylate p53 on serine 46, thereby favoring the transactivation of p53 target genes such as that encoding the cyclin-dependent kinase inhibitor p21 and those that code for several pro-apoptotic effectors. p38 $\alpha$  plays a major role in distinct cell cycle checkpoints including the G<sub>1</sub>/S,<sup>29-32</sup> G<sub>2</sub>/M<sup>24,27,33,34</sup> and the spindle assembly checkpoint,<sup>35</sup> as well as in multiple pro-survival signaling pathways.<sup>36</sup> Driven by these considerations, we investigated whether p38 $\alpha$  might also affect the p53-regulated shift from diploidy to tetraploidy and aneuploidy. Here, we report the unexpected finding that p38 $\alpha$  exerts a major role in the mitotic progression of tetraploid cells in a p53-deficient (but not in a p53-sufficient) context. Thus, p38 $\alpha$  acquires a new role in the regulation of tetraploidy.

## Results and Discussion

**Hyperphosphorylation of p38 $\alpha$  in tetraploid cells.** Using an established protocol,<sup>8,14</sup> we generated a series of tetraploid clones from diploid *p53*<sup>+/+</sup> or isogenic *p53*<sup>-/-</sup> HCT 116 cells. In line with previous reports,<sup>8,23</sup> all *p53*<sup>+/+</sup> tetraploids had a stable phenotype over at least 20 passages, whereas *p53*<sup>-/-</sup> tetraploids either remained stable (~30% of clones) or more frequently (~70% of cases) generated a population with a near-to-diploid DNA content that progressively expanded (see examples of phase 1, P1 and phase 2, P2) (Fig. 1A). Such a genomic instability correlated with a high frequency of multipolar mitose.<sup>23</sup> Unstable *p53*<sup>-/-</sup> tetraploids (but not stable *p53*<sup>+/+</sup> or *p53*<sup>-/-</sup> cells) manifested increased expression of the oncoprotein MOS (Fig. 1B), in accord with previous observations.<sup>23</sup> In addition, we found that *p53*<sup>-/-</sup> tetraploid cells, be them stable or unstable, manifested an increased phosphorylation of p38 $\alpha$  on threonine 180 and tyrosine 182 (compared to normal cells, *p53*<sup>-/-</sup> diploids as well as to *p53*<sup>+/+</sup> tetraploids), as detectable by immunoblotting with a phospho-neoepitope-specific antibody (Fig. 1B). On the other hand, there was no change in the expression level of total (phosphorylated + dephosphorylated) p38 $\alpha$  at the protein level, as determined by western blot (Fig. 1B), nor any major (>25%) change at the mRNA level (Fig. 1C), as determined by microarray-based transcriptome analyses. In conclusion, we observed that p38 $\alpha$  is hyperphosphorylated in *p53*<sup>-/-</sup> tetraploid cells.

**Localization of phosphorylated p38 $\alpha$  on centrosomes and midbodies.** In order to determine whether p38 $\alpha$  phosphorylation is selectively linked to tetraploidy, we purified pseudo-diploid cells (with a chromosomal content of ~2n) or tetraploids (with a chromosomal content of ~8n, in the G<sub>2</sub>/M phase of their cell cycle) by Fluorescence Activated Cell Sorting, FACS, see gates A and B in (Fig. 1A). Immunoblotting revealed that p38 $\alpha$  was not (or only marginally) phosphorylated in recently formed pseudo-diploid cells, underscoring the functional link between

tetraploidy and p38 $\alpha$  phosphorylation. In addition, we observed that tetraploid cells in the G<sub>2</sub>/M phase exhibited a much stronger p38 $\alpha$  phosphorylation than cell populations randomly distributed in the cell cycle (Fig. 1B). Intrigued by this observation, we performed immunofluorescence microscopy of *p53*<sup>-/-</sup> tetraploids and found that phosphorylated p38 $\alpha$  (P-p38 $\alpha$ ) selectively accumulates in mitotic cells. Moreover, we observed that the subcellular localization of p38 $\alpha$  exhibits a cell cycle dependency. During metaphase, P-p38 $\alpha$  localized to centrosomes (staining positively for  $\gamma$ -tubulin), in the context of both normal bipolar mitoses (with a classical metaphase plates organized by two centrosomes) and abnormal multipolar mitoses (with more than two centrosomes and abnormal Y- or X-shaped metaphase figures) (Fig. 1D). In contrast, during telophase, P-p38 $\alpha$  gathered to the single midbody that is generated upon bipolar or multipolar cytokinesis (Fig. 1D). Of note, the immunofluorescence staining observed with the phospho-neoepitope-specific antibody recognizing P-p38 $\alpha$  was specific because no signal was detected when p38 $\alpha$  was depleted with a specific small interfering RNA (siRNA) (Fig. 1D). In conclusion, in *p53*<sup>-/-</sup> tetraploid cells, P-p38 $\alpha$  behaves like a mitotic passenger protein.

**Selective cell cycle effects of p38 $\alpha$  in p53-deficient tetraploids.** We next sought to determine the impact of p38 $\alpha$  on mitotic progression. We employed two distinct but complementary strategies for the inhibition of p38 $\alpha$ , namely p38 $\alpha$  depletion by two non-overlapping siRNAs (Fig. 2A) or pharmacological inhibition of the p38 $\alpha$  enzymatic activity with the chemical agent SB203580. Depletion of p38 $\alpha$  reduced the proliferation in each of the tetraploid clones tested, irrespective of their p53 status, by approximately 20% (Fig. 2B). However, depletion or inhibition of p38 $\alpha$  had a specific effect on the cell cycle that depended on p53 status. Thus, while neither the depletion (with two distinct siRNAs) nor the inhibition (with SB203580) of p38 $\alpha$  did influence the cell cycle distribution of *p53*<sup>+/+</sup> tetraploid cells, p38 $\alpha$  depletion or inhibition resulted in a partial blockage in the G<sub>2</sub>/M phase of their *p53*<sup>-/-</sup> counterparts, as well as in a reduced generation of pseudo-diploid cells (Fig. 2C and D). As a further control of specificity we used SB202474, which is chemically related to SB203580 but does not inhibit p38 $\alpha$ . SB202474 failed indeed to increase the frequency of *p53*<sup>-/-</sup> tetraploids with an ~8n DNA content (Fig. 2D). Driven by these observations, we performed an extensive cell cycle staging to determine the impact of p38 $\alpha$  on the mitotic progression of *p53*<sup>+/+</sup> versus *p53*<sup>-/-</sup> tetraploids. The systematic comparison of mitoses from *p53*<sup>+/+</sup> or *p53*<sup>-/-</sup> tetraploids that were treated with a control siRNA or with a p38 $\alpha$ -depleting siRNA revealed that the spindle assembly checkpoint (defined by the presence of BUBR1 at kinetochores)<sup>37</sup> was activated in most *p53*<sup>-/-</sup> (but not in *p53*<sup>+/+</sup>) tetraploids upon p38 $\alpha$  depletion (Fig. 2E). We found that p38 $\alpha$  depletion (Fig. 2F) or inhibition (not shown) increased the mitotic index of *p53*<sup>-/-</sup> (but not *p53*<sup>+/+</sup>) tetraploid cells, while reducing the anaphase-to-telophase ratio, two signs of metaphase blockage. In addition, we found that the knockdown of p38 $\alpha$  increased the frequency of abnormal bipolar (exhibiting misaligned or lagging chromosomes) and monopolar metaphases. In contrast, the frequency of multipolar divisions (which are detectable among unstable but not among

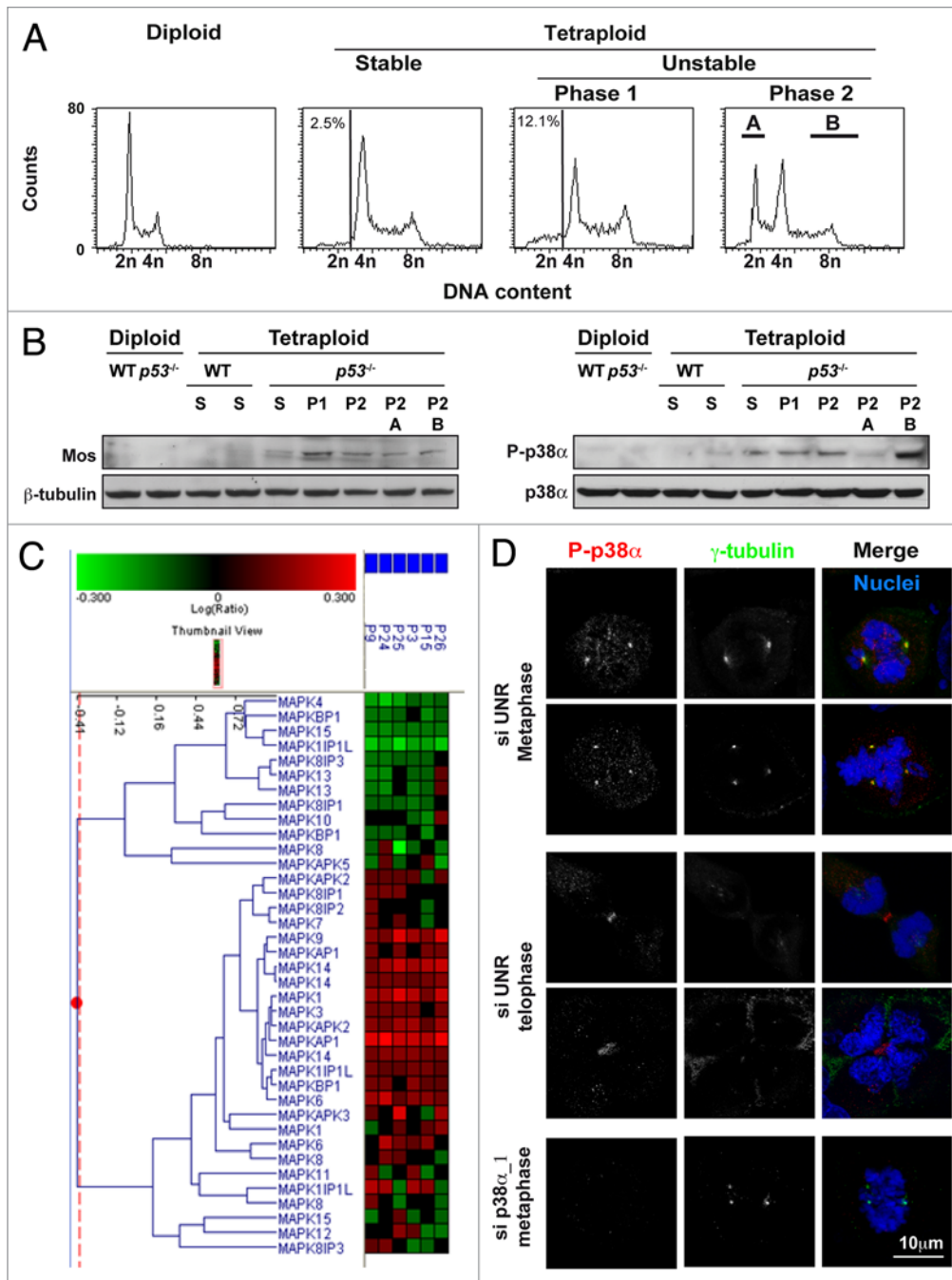


**Figure 1.** For figure legend, see page 2825.

stable *p53*<sup>-/-</sup> tetraploid cells) was reduced by siRNA-mediated p38α downregulation (Fig. 2F). Thus, the depletion/inhibition of p38α has a major effect on the mitotic progression of *p53*<sup>-/-</sup> but not *p53*<sup>+/+</sup> tetraploid cells.

**Concluding remarks.** In the present study, we revealed a hitherto unexpected, selective role of p38α in the mitotic progression of *p53*<sup>-/-</sup> but not *p53*<sup>+/+</sup> tetraploids. p38α was indeed hyperphosphorylated in *p53*<sup>-/-</sup> but not in *p53*<sup>+/+</sup> tetraploid cells. This hyperphosphorylation occurred mostly in mitosis, when P-p38α behaved like a passenger protein, preferably localizing to centrosomes during metaphase and to the midbody during telophase.

Accordingly, inhibition or depletion of p38α had a drastic effect on mitosis in *p53*<sup>-/-</sup> but not in *p53*<sup>+/+</sup> tetraploids. Only in *p53*<sup>-/-</sup> tetraploids, p38α depletion did result in the systematic induction of the spindle assembly checkpoint coupled to a metaphase arrest, abnormal bipolar metaphases and frequent attempts of monopolar division.

Intriguingly, p38α depletion led to a strong decrease in multipolar divisions, which were frequent among unstable (but not stable) *p53*<sup>-/-</sup> tetraploids, reducing them down to the levels of stable *p53*<sup>-/-</sup> tetraploid cells. This contrasted with the increase in

**Figure 1 (See previous page).** Activation and subcellular localization of p38 $\alpha$ . (A and B) p38 $\alpha$  hyperphosphorylation in p53-deficient tetraploid clones. Representative cell cycle distributions (upon gating on events characterized by normal forward and side scatter parameters) of p53<sup>-/-</sup> diploid and tetraploid cells (A). Tetraploid clones were classified according to their level of genomic instability (as evaluated by the quantification of viable sub-tetraploid populations) in stable (sub-tetraploid cells < 5%) or unstable (sub-tetraploid cells >10%). Unstable clones were further subdivided into “phase 1” and “phase 2” clones, depending on the presence of a broad or a sharp sub-tetraploid peak, respectively. X-axis = propidium iodide (PI) fluorescence (DNA content); Y-axis = cell number per channel (counts). Numbers indicate the percentage of sub-tetraploid cells. In (B) protein extracts from wild type (WT) or p53<sup>-/-</sup> clones of the indicated type (S = stable, P1 = phase 1, P2 = phase 2) were subjected to immunoblotting with antibodies that specifically recognize MOS,  $\beta$ -tubulin, p38 $\alpha$  and phospho-p38 $\alpha$  (P-p38 $\alpha$ ). Immunoblotting was also executed on protein extracts obtained from pseudo-diploid (P2 A) or tetraploid (P2 B) cells purified from a phase 2 unstable clone by cytofluorometry as illustrated in (A) (gates A and B). (C) Microarray analyses of the transcriptome of p53<sup>-/-</sup> tetraploid HCT116 clones. The expression of mitogen-activated protein kinase (MAPK) family members was evaluated in stable (P9, P24 and P25) and unstable (P3, P15 and P26) p53<sup>-/-</sup> tetraploid clones, as compared to pooled tetraploid p53<sup>+/+</sup> clones (W33, W43 and W54). Red and green indicate upregulation and downregulation, respectively, as compared to the reference sample. (D) Phosphorylated p38 $\alpha$  behaves as a mitotic passenger protein. Unstable p53<sup>-/-</sup> tetraploid HCT 116 cells were transfected with a control (siUNR) or a p38 $\alpha$ -specific (sip38 $\alpha$  1) siRNA for 48 h and then subjected to immunofluorescence staining for the simultaneous detection of phosphorylated p38 $\alpha$  (P-p38 $\alpha$ ) and  $\gamma$ -tubulin (green and red fluorescence, respectively). Nuclei were counterstained with Hoechst 33342 (emitting in blue). Representative immunofluorescence microphotographs are shown for cells exhibiting bipolar (upper) or multipolar (bottom) metaphase and telophase. Yellow dots that result from the overlap of green and red fluorescence signals suggest that P-p38 $\alpha$  and  $\gamma$ -tubulin co-localize at centrosomes in metaphase of cells transfected with siUNR (scale bar = 10  $\mu$ m). Single-channel microphotographs for both the green and red fluorescence channel are provided.

the frequency of multinucleated cells that was induced by p38 $\alpha$  downregulation in both stable and unstable p53<sup>-/-</sup> tetraploids. At present, we have no complete explanation for this effect. However, it is tempting to speculate that the absence of p38 $\alpha$  might negatively affect centrosome duplication, maturation or separation, thereby favoring the occurrence of monopolar or bipolar divisions over multipolar ones. Alternatively or in addition, the inhibition of p38 $\alpha$  might increase the probability of centrosome aggregation as a result of the continued activation of the spindle assembly checkpoint, resulting in the prolongation of the metaphase time. Mitotic failure with completed karyokinesis yet absent cytokinesis then might explain the increment in the frequency of multinucleated cells.

As evoked in the Introduction to this paper, a large body of literature generated on diploid cells indicates that p38 $\alpha$  contributes to the execution of cell cycle checkpoints by phosphorylating and activating p53.<sup>29,32,36,38,39</sup> We have ourselves contributed to this paradigm by showing that recombinant purified p38 $\alpha$  can phosphorylate p53 on serine 46<sup>40</sup> and by demonstrating that inhibition of the checkpoint kinase 1 (CHK1) can activate p53 through p38 $\alpha$  in tetraploid cancer cells, thereby causing apoptosis.<sup>41</sup> In stark contrast, the results shown here indicate that p38 $\alpha$  can be overactivated in a p53-deficient context and that p38 $\alpha$  plays a major role in facilitating cell cycle progression in the absence of p53. At present, we ignore the precise downstream effectors of p38 $\alpha$  in this setting, although the Polo-like kinase 1 (PLK1, which can be phosphorylated by MK2, a MAPK that is subjected to p38 $\alpha$ -mediated regulation)<sup>42</sup> and the phosphatase CDC25B<sup>24,43</sup> are possible candidates. Irrespective of these details, our results indicate that p38 $\alpha$  has a major function in the mitotic progression of p53<sup>-/-</sup> tetraploid cells.

## Materials and Methods

**Cell lines, culture conditions and chemicals.** Tetraploid HCT 116 colon carcinoma cells were generated from both wild type (WT, p53<sup>+/+</sup>) and p53<sup>-/-</sup> diploid parental cells (kindly provided by Bert Vogelstein, Sidney Kimmel Comprehensive Cancer Center, Baltimore, USA), and routinely tested for p53 status by

immunoblotting. Cells were maintained in McCoy's 5A medium supplemented with 10% fetal calf serum (FCS) at 37°C in a 5% CO<sub>2</sub> atmosphere and seeded onto the appropriate supports for cell culture (6-, 12-, 24- or 96-well plates, 35 or 100 mm Petri dishes) 24 h before the beginning of experiments. For each experiment, at least three different clones for each genotype and/or phenotype were used. The p38 $\alpha$  inhibitor SB203580 and the inactive chemically-related compound SB202474 were purchased from Merck Chemicals (Nottingham, UK). Stock solutions were prepared following the manufacturer's recommendations. Unless otherwise indicated, media and supplements for cell culture were purchased from Gibco-Invitrogen (Carlsbad, USA) and plasticware from Corning B.V. Life Sciences (Schiphol-Rijk, The Netherlands).

**Cytofluorometric studies.** For the quantification of DNA content (cell cycle profiling) and cell sorting, live cells were collected and stained with 2  $\mu$ M Hoechst 33342 (Molecular Probes-Invitrogen). Alternatively, to assess cell cycle distribution, cells were collected, fixed by gentle vortexing in ice-cold 80% (v/v) ethanol (Carlo Erba Reagents, Milano, Italy) and stained with 50  $\mu$ g/mL propidium iodide (PI) in 0.1% D-glucose (w/v in PBS) supplemented with 1  $\mu$ g/mL (w/v) RNase A.<sup>44</sup> Cell proliferation was measured by the fluorescein-based dye 5-(and-6)-carboxy-fluorescein diacetate succinimidyl ester (CFSE, from Molecular Probes-Invitrogen). Briefly, 1 x 10<sup>6</sup> cells were incubated with 25  $\mu$ M CFSE in PBS for 10 min at 37°C. The labeling reaction was stopped by adding an equal volume of FCS and 5 x 10<sup>4</sup> cells were seeded in 12-well plates. Twenty-four hours later, cells were transfected with small interfering RNA (siRNAs, see below) and grown in culture for additional 3 to 5 days, and cell proliferation monitored daily by cytofluorometry. Cytofluorometric acquisitions were performed on a FACSCalibur or a FACScan cytofluorometer (BD Biosciences) equipped with a 70  $\mu$ m nozzle. Statistical analysis was performed by using the CellQuest™ software (BD Biosciences), upon gating on the events characterized by normal forward scatter and side scatter parameters.

**Microarray analyses.** Total RNA was extracted and processed as previously described,<sup>45</sup> labeled with Cyanine 5 and Cyanine 3 according to a dual color method that allows for the

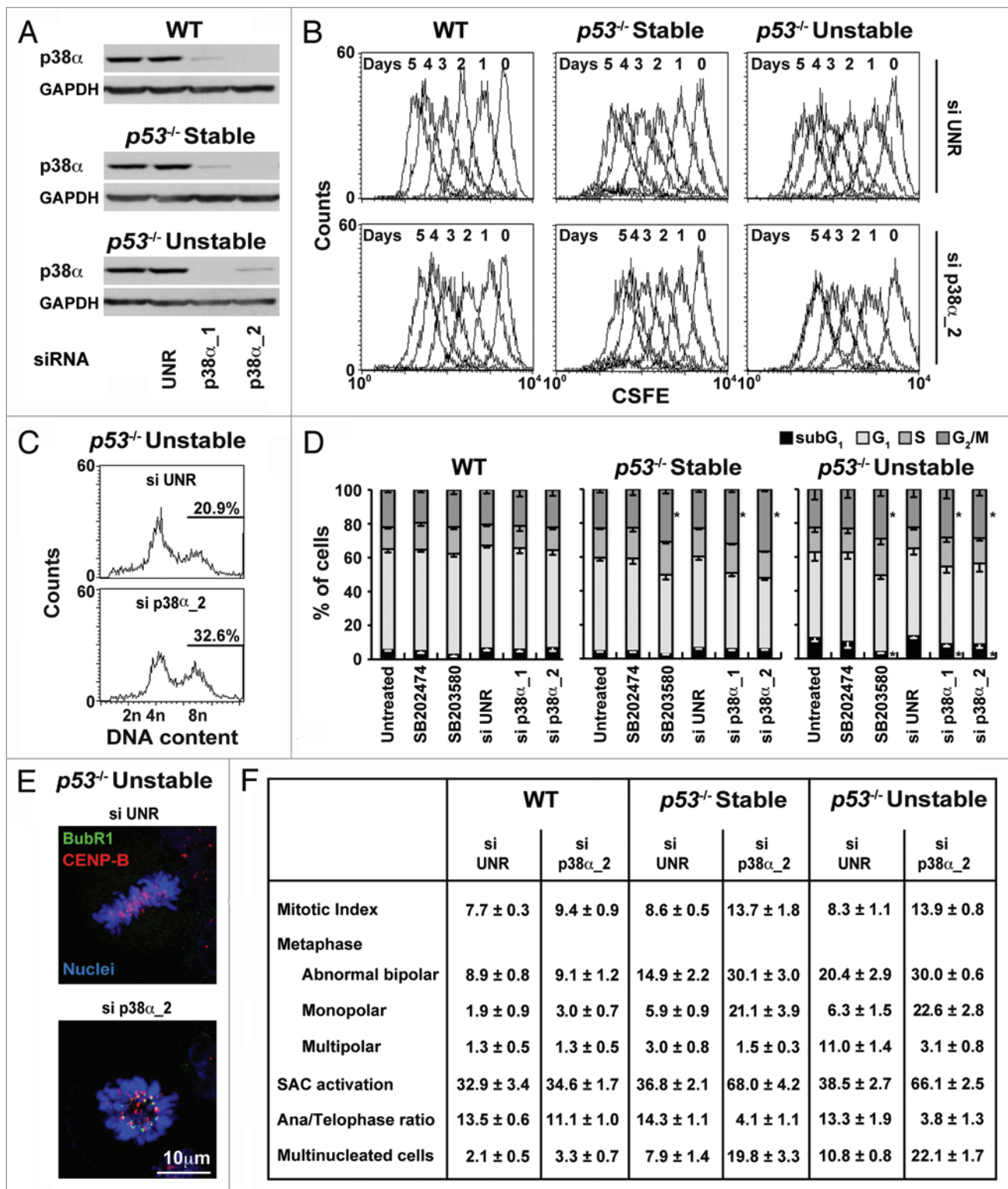


**Figure 2.** For figure legend, see page 2828.

discrimination between the probes from experimental samples and those from the reference condition<sup>8</sup> and then hybridized to G4112F 4 x 44K Agilent Human oligonucleotide microarrays (Agilent Technologies, Santa Clara, USA). A set of 6 dye-swapped experiments was performed to compare (in each single

experiment) the mRNA transcriptome of *p53*<sup>-/-</sup> tetraploid HCT 116 clones (specimens) to that from pooled tetraploid WT clones (reference). From each of the 6 combined experiments, signatures (list of accession numbers) at p values <10<sup>-5</sup> were extracted and annotated with the most updated version of Entrez Gene

**Figure 2 (See previous page).** Effects of p38 $\alpha$  in the mitotic progression of p53-deficient tetraploid cells. (A) Efficacy of siRNA-mediated depletion of p38 $\alpha$ . Wild type (WT) or stable and unstable phase 1 p53<sup>-/-</sup> tetraploid HCT 116 cells were transfected with a control siRNA (siUNR) or with siRNAs specific for p38 $\alpha$  (sip38 $\alpha_1$  and sip38 $\alpha_2$ ) for 48 h, followed by protein extraction and immunoblotting with antibodies that recognize p38 $\alpha$  and glyceraldehyde-3-phosphate dehydrogenase (GAPDH, monitored as a loading control). (B) p38 $\alpha$  depletion affects the proliferation of tetraploid cells. Stable (WT and p53<sup>-/-</sup>) and unstable p53<sup>-/-</sup> tetraploid HCT 116 clones were labeled with 5-(and-6)-carboxyfluorescein diacetate succinimidyl ester (CFSE) for 24 h and then transfected with a control (siUNR) or a p38 $\alpha$ -specific (sip38 $\alpha_2$ ) siRNA, followed by daily assessment of cell proliferation by cytofluorometry. Day 0 = transfection day. Fluorescence histograms are representative of three independent experiments with similar results. (C and D) Effects of p38 $\alpha$  inactivation and depletion on cell cycle distribution. HCT 116 cell clones of the indicated type were left untreated, treated with 1  $\mu$ M SB203580 (a p38 $\alpha$  inhibitor) or 1  $\mu$ M SB 202474 (a compound chemically related to SB203580 that does not inhibit p38 $\alpha$ ) or transfected with a control (siUNR) or a p38 $\alpha$ -specific (sip38 $\alpha_2$ ) siRNA for 72 h followed by DNA content analysis. Representative cell cycle distributions of siUNR- versus sip38 $\alpha_2$ -transfected cells are shown in (C) X-axis = propidium iodide (PI) fluorescence (DNA content); Y-axis = cell number per channel (counts). Numbers indicate the percentage of cells in the G<sub>2</sub>-M phase of the cell cycle. Quantitative data are reported in (D) Columns depict the percentage of cells characterized by sub-G<sub>1</sub>, G<sub>1</sub>, S and G<sub>2</sub>/M DNA content (mean  $\pm$  SEM, n = 5 independent determinations). Asterisks indicate statistically significant differences between data from untreated versus treated or siUNR-transfected versus sip38 $\alpha_2$ -transfected cells (Student's t-test, p < 0.05). (E and F) p38 $\alpha$  depletion promotes mitotic arrest in p53<sup>-/-</sup> HCT 116 tetraploid cells. HCT 116 clones of the indicated type were transfected with a control siRNA (siUNR) or a siRNA specific for p38 $\alpha$  (sip38 $\alpha_2$ ) for 72 h. Thereafter, cells were processed for immunofluorescence microscopy-based detection of spindle assembly checkpoint (SAC) activation, as monitored by the localization at kinetochore of BUBR1 (green fluorescence). Centromeres were visualized with an antibody that recognizes CENP-B, a structural component of the kinetochore (red fluorescence). Alternatively, cells were subjected to immunofluorescence staining for the simultaneous detection of  $\beta$ - and  $\gamma$ -tubulin. In (F) representative images of SAC activation upon p38 $\alpha$  depletion in p53<sup>-/-</sup> HCT 116 tetraploid cells are shown (scale bar = 10  $\mu$ m). Hoechst 33342 (emitting in blue) was employed as nuclear counterstain. Quantitative data relative to the indicated mitotic parameters are reported in (F) (mean  $\pm$  SEM, n = 4).

(NCBI, Bethesda, USA, <http://www.ncbi.nlm.nih.gov/gene>). Genes belonging to the MAPK family were defined by means of the Ingenuity Pathways Analysis software (Ingenuity, Mountain View, USA, [http://www.ingenuity.com/products/pathways\\_analysis.html](http://www.ingenuity.com/products/pathways_analysis.html)).

**Transfections and RNA interference.** The knockdown of p38 $\alpha$  was performed either with a commercial siRNA (siGENOME Smart-pool M-003512, p38 $\alpha_1$ ) purchased from Dharmacon Inc., (Chicago, USA) or with a custom-designed siRNA duplex (p38 $\alpha_2$ , sense: 5'-GCA AGA AAC UAU AUU CAG UdT dT-3'),<sup>46</sup> purchased from Sigma-Proligo (The Woodlands, USA). A non-targeting siRNA with a sequence unrelated to both human and murine genomes (siUNR, sense 5'-GCC GGU AUG CCG GUU AAG UdT dT-3') was used as a negative control. HCT 116 cells in 12-well plates were siRNA-transfected at 30–40% confluence by means of the HiPerFect<sup>®</sup> transfection reagent (Qiagen), as previously described.<sup>47</sup> After 72 h, transfection efficiency was determined by immunoblotting (see below).

**Immunoblotting.** HCT 116 cells were detached, washed with cold PBS and lysed in a buffer containing 1% NP40, 20 mmol/L HEPES, 10 mmol/L KCl, 1 mmol/L EDTA, 10% glycerol, 1 mmol/L orthovanadate, 1 mmol/L phenylmethylsulfonyl fluoride, 1 mmol/L DTT + protease inhibitor tablets followed by standard immunoblotting with antibodies specific for MOS (Stressgen, Victoria, Canada), p38 $\alpha$  (Millipore-Chemicon International, Temecula, USA) and phospho-p38 $\alpha$  (Thr180/Tyr182, P-p38 $\alpha$ , from Cell Signaling Technology Inc., Danvers, USA). Primary antibodies that specifically recognize glyceraldehyde-3-phosphate dehydrogenase (GAPDH, from Millipore-Chemicon International) or  $\beta$ -tubulin (Sigma-Aldrich, St. Louis, USA) were used as lane loading controls.

**Immunofluorescence microscopy.** Immunofluorescence microscopy assessments were performed as previously described.<sup>47</sup> Briefly, cells were fixed in 4% paraformaldehyde, PFA, (w/v in PBS), permeabilized with 0.1% SDS and immunostained with antibodies specific for  $\gamma$ - and  $\beta$ -tubulin (both from

Sigma-Aldrich). To detect the localization of BUBR1 at kinetochores, cells were fixed in 4% PFA (w/v in PIPES buffer: 80 mM PIPES, 5 mM EGTA, 2 mM MgCl<sub>2</sub>) for 10 min at room temperature (RT), washed once with PBS and permeabilized in 0.2% (v/v) Triton<sup>®</sup> X-100 (Sigma-Aldrich) in PBS. Unspecific binding sites were saturated with a buffer containing 10 mM Tris pH 7.5, 150 mM NaCl and 0.1% (w/v) BSA in PBS for 15 min at RT, followed by incubation for 1 h at 37°C with primary antibodies against BUBR1 (BD Biosciences) and CENP-B (Santa Cruz Biotechnology, San Jose, USA).<sup>48</sup> To detect the localization of p38 $\alpha$  at centrosomes, cells were fixed in 4% PFA (w/v in PBS) for 15 min at 4°C and permeabilized by subsequent incubation in 0.2% Triton<sup>®</sup> X-100 (v/v in PBS) for 5 min at RT and in 100% methanol (Carlo Erba Reagents) for 10 min at -20°C. Thereafter, cells were pre-incubated in 20% goat serum for 30 min at 37°C in a humidified chamber, and then incubated for 2 h with antibodies that specifically recognize P-p38 $\alpha$  (Thr180/Tyr182, Cell Signaling Technology Inc.,) and/or  $\gamma$ -tubulin (Sigma-Aldrich). Slides were then rinsed in 1% BSA and incubated for 1 h at 37°C with secondary goat anti-rabbit or anti-mouse IgGs conjugated to Alexa Fluor<sup>®</sup> 568 or to Alexa Fluor<sup>®</sup> 488 fluorochromes (emitting in red and in green, respectively; both from Molecular Probes-Invitrogen, Eugene, USA) in 2% BSA (w/v in PBS). Nuclei were counterstained with 10  $\mu$ M Hoechst 33342 (Molecular Probes-Invitrogen). Fluorescence images were captured on an IRE2 microscope equipped with a DC300F camera (both from Leica Microsystems GmbH, Wetzlar, Germany). Confocal microscopy was performed on a LSM 510 microscope (Carl Zeiss MicroImaging GmbH, Oberkochen, Germany) equipped with a 63X objective. Signals from different probes were taken in sequential scan mode and image analysis was performed with the open source software Image J (freely available from the National Institute of Health, Bethesda, USA at the address <http://rsb.info.nih.gov/ij/>).

**Statistical procedures.** Unless otherwise specified, all experiments were performed in triplicate parallel instances and independently repeated at least three times. Data were analyzed with

Microsoft Excel (Microsoft Co., Redmond, USA) and statistical significance was assessed by means of two-tailed Student's *t*-test (\**p* < 0.05).

### Acknowledgements

We are indebted to Bert Vogelstein (John Hopkins University, Baltimore, USA) for the gift of genetically manipulated HCT 116 cells. G.K. is supported by the Ligue Nationale contre le Cancer

(Equipe labellisé), Agence Nationale pour la Recherche (ANR), European Commission (Active p53, Apo-Sys, ChemoRes, ApopTrain), Fondation pour la Recherche Médicale (FRM), Institut National du Cancer (INCa) and Cancéropôle Ile-de-France. M.C. is supported by the Association pour la Recherche sur le Cancer (ARC). I.V. is supported by the Ligue Nationale contre le Cancer, L.S. and SR-V by FRM, L.G. by the Apo-Sys consortium of the European Union.

### References

- Heselmeyer K, Schrock E, du Manoir S, Blegen H, Shah K, Steinbeck R, et al. Gain of chromosome 3q defines the transition from severe dysplasia to invasive carcinoma of the uterine cervix. *Proc Natl Acad Sci USA* 1996; 93:479-84.
- Maley CC, Galipeau PC, Li X, Sanchez CA, Paulson TG, Blount PL, et al. The combination of genetic instability and clonal expansion predicts progression to esophageal adenocarcinoma. *Cancer Res* 2004; 64:7629-33.
- Margolis RL. Tetraploidy and tumor development. *Cancer Cell* 2005; 8:353-4.
- Tighe A, Johnson VL, Taylor SS. Truncating APC mutations have dominant effects on proliferation, spindle checkpoint control, survival and chromosome stability. *J Cell Sci* 2004; 117:6339-53.
- Schlegel BP, Starita LM, Parvin JD. Overexpression of a protein fragment of RNA helicase A causes inhibition of endogenous BRCA1 function and defects in ploidy and cytokinesis in mammary epithelial cells. *Oncogene* 2003; 22:983-91.
- Aylon Y, Michael D, Shmueli A, Yabuta N, Nojima H, Oren M. A positive feedback loop between the p53 and Lats2 tumor suppressors prevents tetraploidization. *Genes Dev* 2006; 20:2687-700.
- Davoli T, Denchi EL, de Lange T. Persistent telomere damage induces bypass of mitosis and tetraploidy. *Cell* 141:81-93.
- Castedo M, Coquelle A, Vivet S, Vitale I, Kauffmann A, Dessen P, et al. Apoptosis regulation in tetraploid cancer cells. *EMBO J* 2006; 25:2584-95.
- Caldwell CM, Green RA, Kaplan KB. APC mutations lead to cytokinetic failures in vitro and tetraploid genotypes in Min mice. *J Cell Biol* 2007; 178:1109-20.
- Dikovskaya D, Schiffmann D, Newton IP, Oakley A, Kroboth K, Sansom O, et al. Loss of APC induces polyploidy as a result of a combination of defects in mitosis and apoptosis. *J Cell Biol* 2007; 176:183-95.
- Cross SM, Sanchez CA, Morgan CA, Schimke MK, Ramel S, Idzerda RL, et al. A p53-dependent mouse spindle checkpoint. *Science* 1995; 267:1353-6.
- Andreassen PR, Lohez OD, Lacroix FB, Margolis RL. Tetraploid state induces p53-dependent arrest of nontransformed mammalian cells in G<sub>1</sub>. *Mol Biol Cell* 2001; 12:1315-28.
- Fujiwara T, Bandi M, Nitta M, Ivanova EV, Bronson RT, Pellman D. Cytokinesis failure generating tetraploids promotes tumorigenesis in p53-null cells. *Nature* 2005; 437:1043-7.
- Castedo M, Coquelle A, Vitale I, Vivet S, Mouhamad S, Viaud S, et al. Selective resistance of tetraploid cancer cells against DNA damage-induced apoptosis. *Ann N Y Acad Sci* 2006; 1090:35-49.
- Senovilla L, Vitale I, Galluzzi L, Vivet S, Joza N, Younes AB, et al. p53 represses the polyploidization of primary mammary epithelial cells by activating apoptosis. *Cell Cycle* 2009; 8:1380-5.
- Wang X, Zhou YX, Qiao W, Tominaga Y, Ouchi M, Ouchi T, et al. Overexpression of aurora kinase A in mouse mammary epithelium induces genetic instability preceding mammary tumor formation. *Oncogene* 2006; 25:7148-58.
- Yin XY, Grove L, Datta NS, Long MW, Prochownik EV. C-myc overexpression and p53 loss cooperate to promote genomic instability. *Oncogene* 1999; 18:1177-84.
- Incassati A, Patel D, McCance DJ. Induction of tetraploidy through loss of p53 and upregulation of Plk1 by human papillomavirus type-16 E6. *Oncogene* 2006; 25:2444-51.
- Storchova Z, Pellman D. From polyploidy to aneuploidy, genome instability and cancer. *Nat Rev Mol Cell Biol* 2004; 5:45-54.
- Roumier T, Valent A, Perfettini JL, Metivier D, Castedo M, Kroemer G. A cellular machine generating apoptosis-prone aneuploid cells. *Cell Death Differ* 2005; 12:91-3.
- Zhivotovskiy B, Kroemer G. Apoptosis and genomic instability. *Nat Rev Mol Cell Biol* 2004; 5:752-62.
- Ganem NJ, Storchova Z, Pellman D. Tetraploidy, aneuploidy and cancer. *Curr Opin Genet Dev* 2007; 17:157-62.
- Vitale I, Senovilla L, Jemaa M, Michaud M, Galluzzi L, Kepp O, et al. Multipolar mitosis of tetraploid cells: inhibition by p53 and dependency on Mos. *EMBO J* 29:1272-84.
- Bulavin DV, Higashimoto Y, Popoff JJ, Gaarde WA, Basur V, Potapova O, et al. Initiation of a G<sub>2</sub>/M checkpoint after ultraviolet radiation requires p38 kinase. *Nature* 2001; 411:102-7.
- Rouse J, Cohen P, Trigon S, Morange M, Alonso-Llamazares A, Zamanillo D, et al. A novel kinase cascade triggered by stress and heat shock that stimulates MAPKAP kinase-2 and phosphorylation of the small heat shock proteins. *Cell* 1994; 78:1027-37.
- Han J, Lee JD, Bibbs L, Ulevitch RJ. A MAP kinase targeted by endotoxin and hyperosmolarity in mammalian cells. *Science* 1994; 265:808-11.
- Dmitrieva NI, Bulavin DV, Fornace AJ Jr, Burg MB. Rapid activation of G<sub>2</sub>/M checkpoint after hypertonic stress in renal inner medullary epithelial (IME) cells is protective and requires p38 kinase. *Proc Natl Acad Sci USA* 2002; 99:184-9.
- Reinhardt HC, Aslanian AS, Lees JA, Yaffe MB. p53-deficient cells rely on ATM- and ATR-mediated checkpoint signaling through the p38<sup>MAPK</sup>/MK2 pathway for survival after DNA damage. *Cancer Cell* 2007; 11:175-89.
- Mikule K, Delaval B, Kaldis P, Jurczyk A, Hergert P, Doxsey S. Loss of centrosome integrity induces p38-p53-p21-dependent G<sub>1</sub>-S arrest. *Nat Cell Biol* 2007; 9:160-70.
- Lavoie JN, L'Allemain G, Brunet A, Muller R, Pouyssegur J. Cyclin D1 expression is regulated positively by the p42/p44<sup>MAPK</sup> and negatively by the p38/HOG<sup>MAPK</sup> pathway. *J Biol Chem* 1996; 271:20608-16.
- Casanovas O, Miro F, Estanyol JM, Itarte E, Agell N, Bachs O. Osmotic stress regulates the stability of cyclin D1 in a p38SAPK2-dependent manner. *J Biol Chem* 2000; 275:35091-7.
- Srsen V, Gnadl N, Dammermann A, Merdes A. Inhibition of centrosome protein assembly leads to p53-dependent exit from the cell cycle. *J Cell Biol* 2006; 174:625-30.
- Manke IA, Nguyen A, Lim D, Stewart MQ, Elia AE, Yaffe MB. MAPKAP kinase-2 is a cell cycle checkpoint kinase that regulates the G<sub>2</sub>/M transition and S phase progression in response to UV irradiation. *Mol Cell* 2005; 17:37-48.
- Mikhailov A, Shinohara M, Rieder CL. The p38-mediated stress-activated checkpoint. A rapid response system for delaying progression through antephasis and entry into mitosis. *Cell Cycle* 2005; 4:57-62.
- Takenaka K, Moriguchi T, Nishida E. Activation of the protein kinase p38 in the spindle assembly checkpoint and mitotic arrest. *Science* 1998; 280:599-602.
- Thornton TM, Rincon M. Non-classical p38 map kinase functions: cell cycle checkpoints and survival. *Int J Biol Sci* 2009; 5:44-51.
- Musacchio A, Salmon ED. The spindle-assembly checkpoint in space and time. *Nat Rev Mol Cell Biol* 2007; 8:379-93.
- Bulavin DV, Saito S, Hollander MC, Sakaguchi K, Anderson CW, Appella E, et al. Phosphorylation of human p53 by p38 kinase coordinates N-terminal phosphorylation and apoptosis in response to UV radiation. *EMBO J* 1999; 18:6845-54.
- She QB, Chen N, Dong Z. ERKs and p38 kinase phosphorylate p53 protein at serine 15 in response to UV radiation. *J Biol Chem* 2000; 275:20444-9.
- Perfettini JL, Castedo M, Roumier T, Andreau K, Nardacci R, Piacentini M, et al. Mechanisms of apoptosis induction by the HIV-1 envelope. *Cell Death Differ* 2005; 12:916-23.
- Vitale I, Senovilla L, Galluzzi L, Criollo A, Vivet S, Castedo M, et al. Chk1 inhibition activates p53 through p38<sup>MAPK</sup> in tetraploid cancer cells. *Cell Cycle* 2008; 7:1956-61.
- Tang J, Yang X, Liu X. Phosphorylation of Plk1 at Ser326 regulates its functions during mitotic progression. *Oncogene* 2008; 27:6635-45.
- Cha H, Wang X, Li H, Fornace AJ Jr. A functional role for p38<sup>MAPK</sup> in modulating mitotic transit in the absence of stress. *J Biol Chem* 2007; 282:22984-92.
- Mouhamad S, Galluzzi L, Zermati Y, Castedo M, Kroemer G. Apaf-1 Deficiency Causes Chromosomal Instability. *Cell Cycle* 2007; 6:3103-7.
- Vitale I, Galluzzi L, Vivet S, Nanty L, Dessen P, Senovilla L, et al. Inhibition of Chk1 kills tetraploid tumor cells through a p53-dependent pathway. *PLoS One* 2007; 2:1337.
- Gao X, Wang H, Sairenji T. Inhibition of Epstein-Barr virus (EBV) reactivation by short interfering RNAs targeting p38 mitogen-activated protein kinase or c-myc in EBV-positive epithelial cells. *J Virol* 2004; 78:11798-806.
- Hoffmann J, Vitale I, Buchmann B, Galluzzi L, Schwede W, Senovilla L, et al. Improved cellular pharmacokinetics and pharmacodynamics underlie the wide anticancer activity of sagopilone. *Cancer Res* 2008; 68:5301-8.
- Vitale I, Antocchia A, Cenciarelli C, Crateri P, Meschini S, Arancia G, et al. Combretastatin CA-4 and combretastatin derivative induce mitotic catastrophe dependent on spindle checkpoint and caspase-3 activation in non-small cell lung cancer cells. *Apoptosis* 2007; 12:155-66.